Supplementary Information (SI) for ChemComm.
This journal is © The Royal Society of Chemistry 2026

Supplementary Information

Experimental section

Materials: Urea ($CO(NH_2)_2$), hydrochloric acid (HCl), Nafion (5 wt.%), ammonium fluoride (NH_4F), ruthenium oxide (RuO_2), nickel sulfate hexahydrate ($NiSO_4 \cdot 6H_2O$), sodium dihydrogen phosphate dihydrate ($NaH_2PO_4 \cdot 2H_2O$), sodium phosphate dibasic dodecahydrate ($Na_2HPO_4 \cdot 12H_2O$), ethylenediaminetetraacetic acid disodium ($C_{10}H_{18}N_2Na_2O_8$), N,N-diethyl-p-phenylenediamine ($C_{10}H_{16}N_2$) and iron nitrate nonahydrate ($Fe(NO_3)_3 \cdot 9H_2O$) was obtained from Aladdin Industrial Co., Ltd. Sodium chloride (NaCl), Hydrochloric acid (HCl), ethyl alcohol (C_2H_5OH), potassium hydroxide (KOH), and sodium carbonate (Na_2CO_3) were obtained from Chengdu Kelong Chemical Reagent Factory. All reagents used in this work were analytical grade without further purification. Nickel foam (NF) was obtained from the Wuhan Instrument Surgical Instruments business in Hongshan District. Deionized water (resistivity: 18.3 MΩ·cm) used throughout experiments was purified through a Millipore system.

Synthesis of Sulfate intercalated NiFe layered double hydroxide on NF (S-NiFe LDH/NF): Firstly, well-cut small piece of NF (2.0 × 3.0 cm^2) was sonicated in 3 M HCl, ethanol, and deionized water, respectively for 10 min. Then, they were treated in concentrated hydrochloric acid for 10 minutes to improve the hydrophilicity of the catalyst. Finally, the pretreatment was completed by ultrasonic cleaning in deionized water for 10 minutes. A mixed solution of 1 M $NiSO_4$ and 1 M $Fe(NO_3)_3$ with a volume of 50 mL was prepared. The treated nickel foam was immersed in the above solution and stirred at a rate of 150 rpm overnight. The prepared catalyst was designated as S-NiFe LDH/NF.

Synthesis of NiFe LDH/NF: The NF was treated as same way. Meanwhile, 38 mL DI water was used to dissolve $Fe(NO_3)_3 \cdot 9H_2O$ (1 mmol), urea (10 mmol), $Ni(NO_3)_2 \cdot 6H_2O$ (2 mmol), and NH_4F (4 mmol). The solution and pre-treated NF were then put into a Teflon autoclave and kept 120 °C for six hours. The NF supported with NiFe LDH was treated with DI water and ethanol and dried overnight (60 °C).

Synthesis of RuO_2 on NF: 5 mg RuO_2 powder added in a solution containing 30 μL of Nafion, 485 μL of ethanol, and 485 μL of deionized water with the aid of ultrasonication (30 min) to form a homogeneous ink (5 mg mL^{-1}). Subsequently, 100 μL of the prepared slurry was loaded onto clean NF (0.5 cm × 0.5 cm) with a loading mass of 0.5 mg.

Characterizations: X-ray diffraction (XRD) patterns were recorded on Shimadzu LabX XRD-6100 diffractometer with a Cu Kα radiation (40 kV, 30 mA) of wavelength 0.154 nm (SHIMADZU, Japan). Scanning electron microscopy (SEM) images were obtained on Zeiss Gemni SEM 300, while transmission electron microscopy (TEM) images were taken using a Hitachi H-8100 microscope at 200 kV. The X-ray photoelectron spectra (XPS) measurements were performed on an ESCALABMK II spectrometer using an Mg as the exciting source. Energy dispersive X-ray (EDX) images were acquired on a JEM-2800 electron microscope (JEOL, Japan) operated at 200 kV.

Electrochemical measurements: The standard three-electrode electrochemical analyzer system (CHI 660E, CHI Instruments, China) was used for the electrochemical measurements, using the materials supported on the substrate as working electrodes directly. Commercial graphite rod and Hg/HgO with 1.0 M KOH as the inner reference electrolyte served as the counter electrode and reference electrode, respectively. To exclude the influence of the oxidation peak of Ni^{2+} to Ni^{3+} on the catalytic current density to obtain reliable overpotential calculations, we used linear sweep voltammetry backward scans (from positive to negative direction) for the polarization curves in OER. By using the Nernst equation, the potential versus Hg/HgO was converted to the reversible hydrogen electrode (RHE) scale: E (vs. RHE) = E (vs. Hg/HgO) + 0.098 + 0.059 × pH. Three different electrolytes, including 1 M KOH, 1 M KOH + 0.5 M NaCl, and 1 M KOH + seawater, were used, and the pH was about 14. All the LSV curves were *iR* compensated. EIS was obtained at the open circuit potential from 10000 to 0.01 Hz at an amplitude of 5 mV. The double-layer capacitance values were measured by cyclic voltammetry (CV) at different scan rates

of 10-80 mV s^{-1} in 1 M KOH. The Faradaic efficiency (FE) of OER was determined using the drainage method in a two-compartment H-type cell, which was separated by a Nafion 117 membrane.

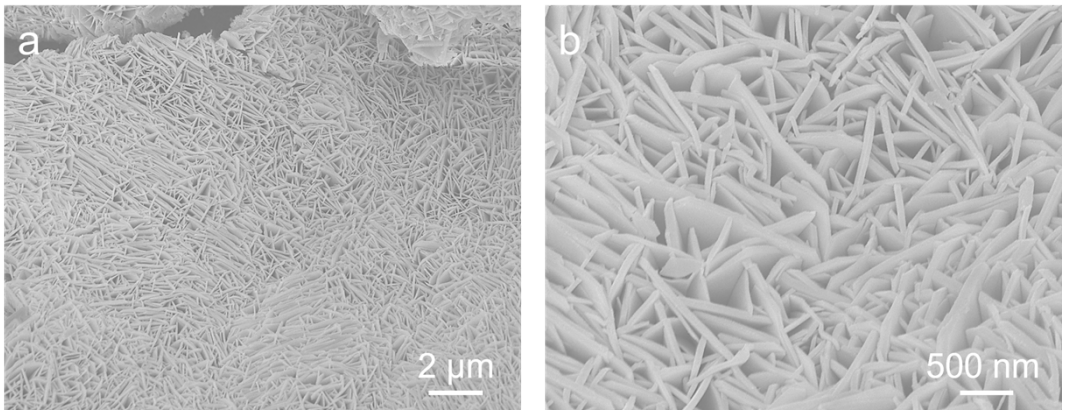

Fig. S1. (a) Low- and (b) high-magnification SEM image of NiFe LDH/NF.

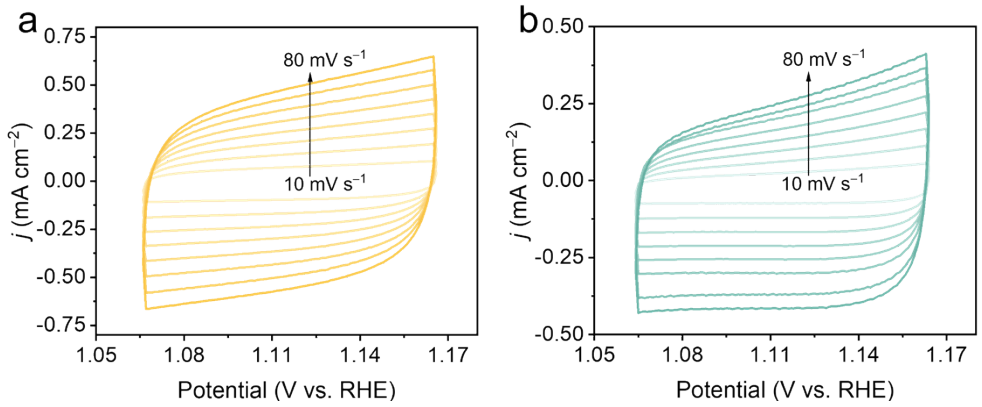

Fig. S2. CV curves of (a) S-NiFe LDH/NF and (b) NiFe LDH/NF in the double-layer region at different scan rates of 10, 20, 30, 40, 50, 60, 70, and 80 mV s^{-1} in 1 M KOH.

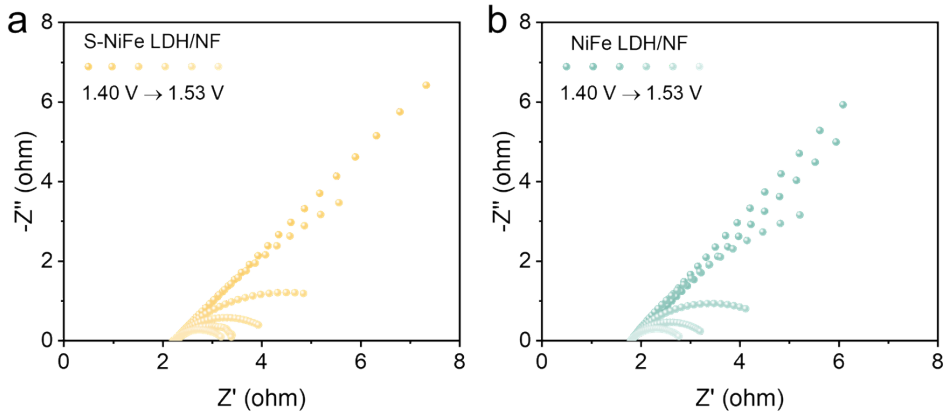

Fig. S3. Nyquist plots at various voltages of (a)S-NiFe LDH/NF and (b) NiFe LDH/NF.

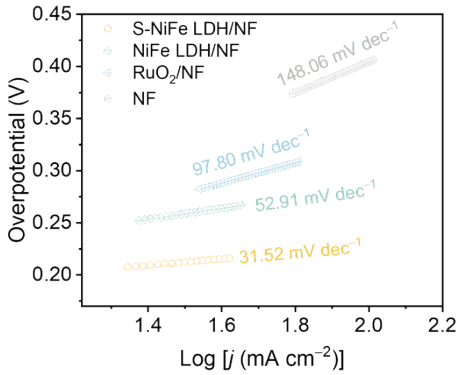

Fig. S4. Tafel plots of S-NiFe LDH/NF, NiFe LDH/NF, RuO_2/NF, and NF in 1 M KOH + seawater.

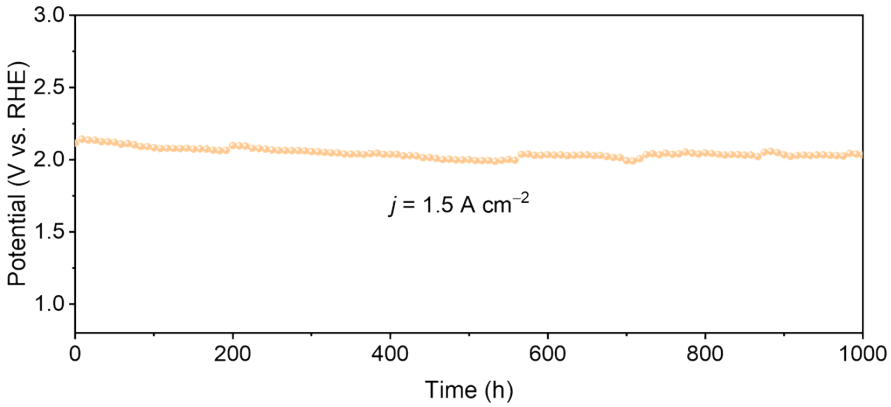

Fig. S5. Chronopotentiometry test of S-NiFe LDH/NF without iR correction in 1 M KOH + seawater.

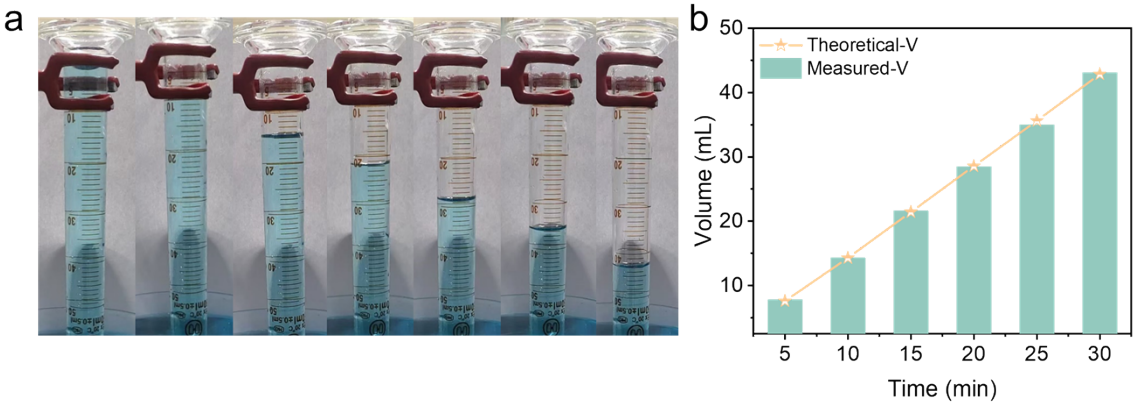

Fig. S6. (a) Digital photographs of the collected O_2 during alkaline seawater oxidation process. (b) Comparison between the amount collected experimentally and calculated O_2 for S-NiFe LDH/NF theoretically at a *j* of 1.5 A cm^{-2} in 1 M KOH + seawater.

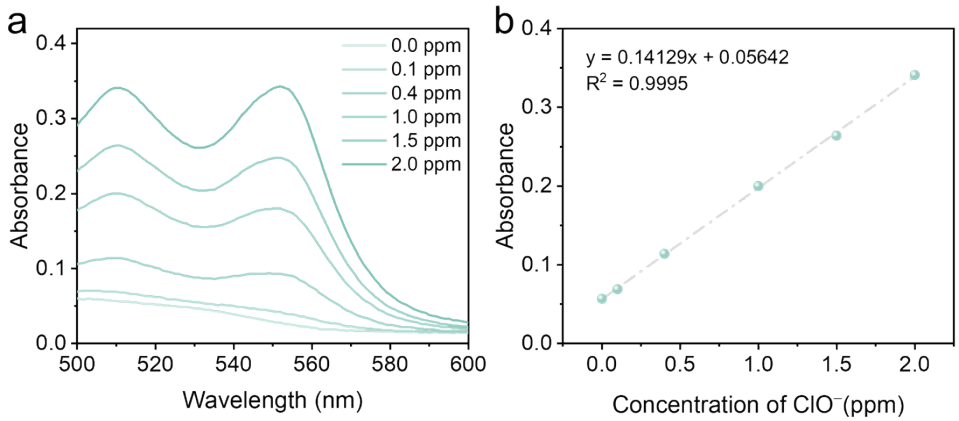

Fig. S7. (a)UV-vis absorption spectra of various active chlorine concentrations, and (b) the corresponding linear fit.

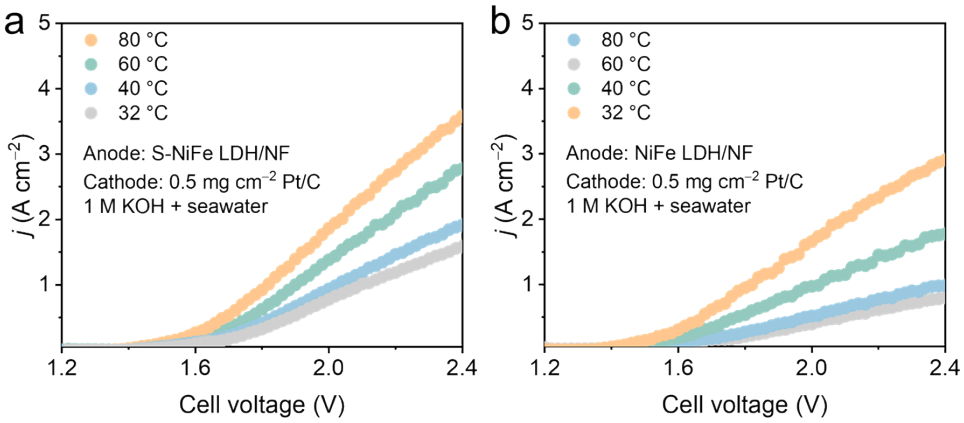

Fig. S8. LSV curves of different anodes (a)S-NiFe LDH/NF and (b) NiFe LDH/NF in AEM electrolyzer.

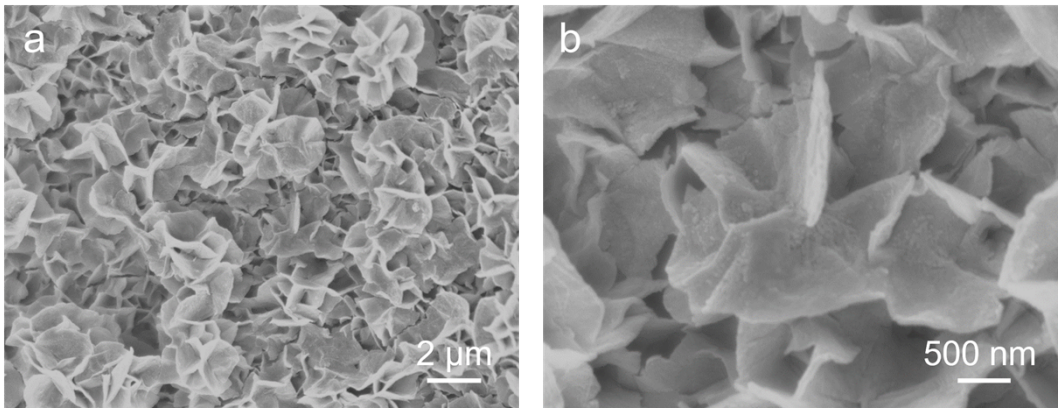

Fig. S9. (a) Low- and (b) high-magnification SEM images of S-NiFe LDH/NF after OER stability test in 1 M KOH + seawater.

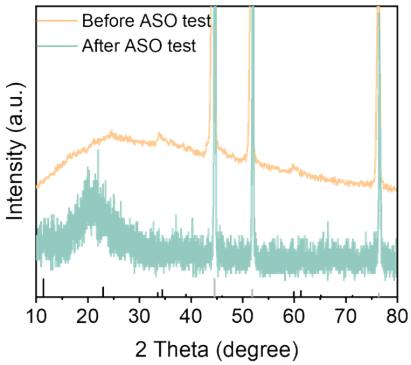

Fig. S10. XRD patterns of S-NiFe LDH/NF before and after OER stability test in 1 M KOH + seawater.

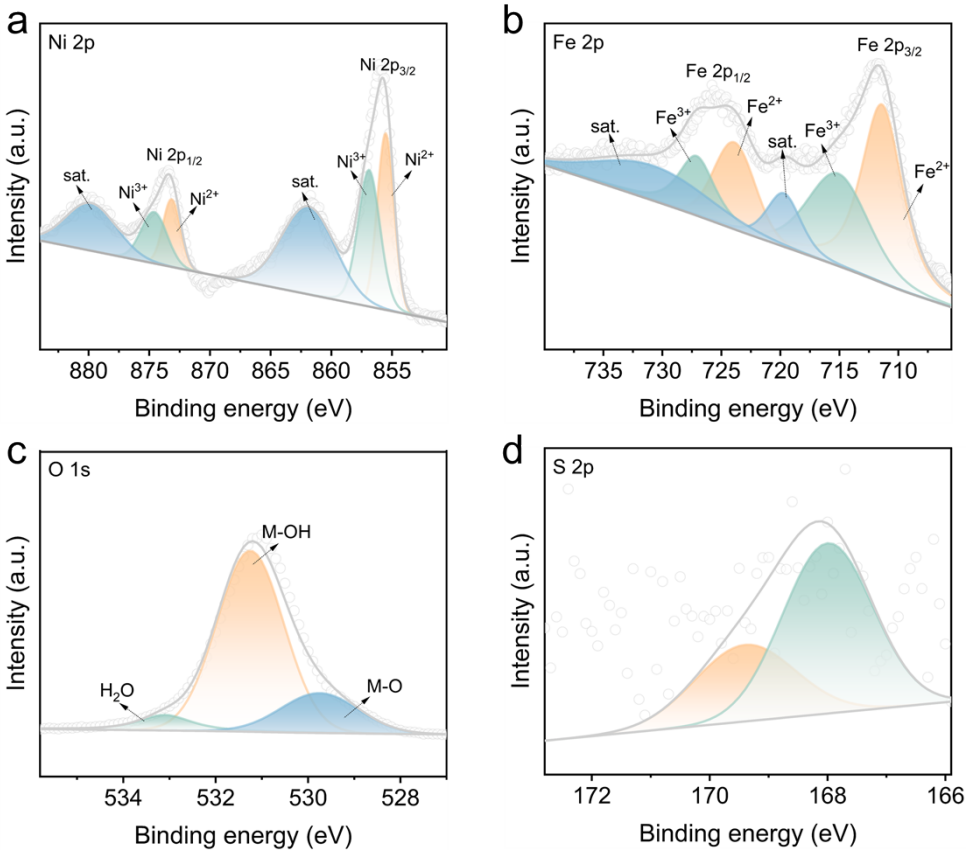

Fig. S11. XPS high resolution spectra in the (a) Ni 2p, (b) Fe 2p, (c) O 1s, and (d) S 2p regions of S-NiFe LDH after stability test.

Table S1 Comparison of the OER catalytic performance of S-NiFe LDH/NF other reported electrocatalysts.

Catalyst	Current density ($mA\ cm^{-2}$)	Overpotential (mV)	Electrolyte	Ref.
S-NiFe LDH/NF	100 500	294 391	1 M KOH + seawater	This work
TS-NiFe-LDH/CC	500 1000	344 412	1 M KOH + seawater	1
Fe-NiS/NF	500 1000	360 440	1 M KOH + seawater	2
Ni_2P-Fe_2P/NF	100 1000	305 431	1 M KOH + seawater	3
Fe_2O_3/NiO/NF	100 500	231 533	1 M KOH + seawater	4
$Ni(TCNQ)_2$/GP	500	550	1 M KOH + seawater	5
Ru-CoO_x/NF	100 500	370 570	1 M KOH + seawater	6
Cr-CoCH/NF	100 500	394 450	1 M KOH + seawater	7
BZ-NiFe LDH/CC	500	610	1 M KOH + seawater	8
NiCoHPi@Ni_3N/NF	500	474	1 M KOH + seawater	9
Co-Ni_3S_2/NF	500	443	1 M KOH + seawater	10
$NiSe_2$@NiOOH/NF	500	460	1 M KOH + seawater	11
Ce-NiFe LDH/NF	1000	390	1 M KOH + seawater	12

References

1 H. Wang, Z. Li, S. Hong, C. Yang, J. Liang, K. Dong, H. Zhang, X. Wang, M. Zhang, S. Sun, Y. Yao, Y. Luo, Q. Liu, L. Li, W. Chu, M. Du, F. Gong, X. Sun and B. Tang, *Small*, 2024, **20**, 2311431.

2 C. Yang, K. Dong, L. Zhang, X. He, J. Chen, S. Sun, M. Yue, H. Zhang, M. Zhang, D. Zheng, Y. Luo, B. Ying, Q. Liu, A. M. Asiri, M. S. Hamdy and X. Sun, *Inorg. Chem.*, 2023, **62**, 7976−7981.

3 L. Wu, L. Yu, F. Zhang, B. McElhenny, D. Luo, A. Karim, S. Chen and Z. Ren, *Adv. Funct. Mater.*, 2021, **31**, 2006484.

4 L. Li, G. Zhang, B. Wang, D. Zhu, D. Liu, Y. Liu, S. Yang. *ACS Appl. Mater. Interfaces*, 2021, **13**, 37152–37161.

5 L. Zhang, J. Wang, P. Liu, J. Liang, Y. Luo, G. Cui, B. Tang, Q. Liu, X. Yan, H. Hao, M. Liu, R. Gao and X. Sun, *Nano Res.*, 2022, **15**, 6084–6090.

6 D. Wu, D. Chen, J. Zhu, S. Mu, *Small*, 2021, **17**, 2102777.

7 M. Zhang, X. He, K. Dong, H. Zhang, Y. Yao, C. Yang, M. Yue, S. Sun, Y. Sun, D. Zheng, Y. Luo, Q. Liu, N. Li, B. Tang, J. Liu and X. Sun, *Chem. Commun.*, 2023, **59**, 9750–9753.

8 L. Zhang, J. Liang, L. Yue, K. Dong, J. Li, D. Zhao, Z. Li, S. Sun, Y. Luo, Q. Liu, G. Cui, A. A. Alshehri, X. Guo and X. Sun, *Nano Res. Energy*, 2022, **1**, e9120028.

9 H. Sun, J. Sun, Y. Song, Y. Zhang, Y. Qiu, M. Sun, X. Tian, C. Li, Z. Lv and L. Zhang, *ACS Appl. Mater. Interfaces*, 2022, **14**, 22061–22070.

10 M. Yue, X. He, S. Sun, Y. Sun, M. S. Hamdy, M. Benaissa, A. A. M. Salih, J. Liu and X. Sun, *Nano Res.*, 2024, **17**, 1050–1055.

11 H. Zhang, X. He, K. Dong, Y. Yao, S. Sun, M. Zhang, M. Yue, C. Yang, D. Zheng, Q. Liu, Y. Luo, B. Ying, S. Alfaifi, X. Ji, B. Tang and X. Sun, *Mater. Today Phys.*, 2023, **38**, 101249.

12 Y. Yao, S. Sun, H. Zhang, Z. Li, C. Yang, Z. Cai, X. He, K. Dong, Y. Luo, Y. Wang, Y. Ren, Q. Liu, D. Zheng, W. Zhuang, B. Tang, X. Sun, W. Hu, *J. Energy Chem.*, 2024, **91**, 306−312.